REDUCTION OF SEISMIC WAVE ENERGY OF SH PULSE BY NONLINEAR SOIL

Vlado Gičev
Univ. of Goce Delčev, Dept. of Computer Science, 2000 Štip, R. Macedonia

Mihailo D. Trifunac and Maria I. Todorovska
Univ. of Southern California, Dept. of Civil Eng., Los Angeles, CA 90089, USA

SUMMARY
Two-dimensional models of a building on a rectangular, flexible foundation in nonlinear soil are analyzed. The building is assumed to be linear, but the foundation and the soil can experience nonlinear deformations. It is shown that the wave energy dissipated during the development of nonlinear strains in the soil can consume a significant part of the input wave energy, and thus less energy is available for excitation of the building. The results help explain why, during the 1994 Northridge earthquake in California, the damage to residential buildings in the areas that experienced large strains in the soil was absent or significantly reduced. The results also suggest major advantages that result from the designs that consider nonlinear soil response.

Keywords: Nonlinear soil-structure interaction; nonlinear waves in the soil and in the foundation.

1. INTRODUCTION

Spatial separation of damaged buildings and of pipe breaks in the near field during the 1994 Northridge, California (Trifunac and Todorovska 1998) and the 1933 Long Beach, California (Trifunac 2003) earthquakes emphasizes the need to understand the nature of the nonlinear responses of soils near the ground surface and their relationship to the soil-structure interaction (SSI). An almost complete absence of damaged buildings in the heavily shaken areas, where soil experienced large nonlinear strains and deformations, suggests that some soils can absorb the energy of incident seismic waves and act as a large-scale natural isolation systems. Since the areas where this energy absorption takes place recurred during two consecutive earthquakes (Trifunac and Todorovska 2004), the associated nonlinear phenomena appear to be associated with the local site characteristics, which do not change for decades, and which therefore could be used, with essentially no additional cost, in the design of structures and in the more advanced approaches to seismic zoning (Trifunac 2008).

The zones where buildings were damaged during the 1994 Northridge earthquake, or where pipes were broken (Trifunac and Todorovska 1997a,b), are not associated with obvious and easily identifiable differences in the amplitudes of recorded peak accelerations, peak velocities, or spectral amplitudes of strong ground motion (Trifunac et al. 1994; 1996; Todorovska and Trifunac 1997a,b), and more subtle and detailed site investigations are required to identify them. These investigations will require detailed and multi-parametric site characterizations that combine the physical properties of the site with the level of its water table and liquefaction susceptibility (Todorovska and Trifunac 1998; Trifunac 1995). The classical earthquake engineering approach correlates damage to structures with the largest relative response of the equivalent single-degree-of-freedom system, in a formulation that is typically based only on the largest peak of the relative response. While this approach can be refined to involve many of the largest peaks of the relative response in the near field of strong ground shaking

(Gupta and Trifunac 1988), it appears that the damage is governed more by the strong pulses that emanate from the broken asperities on the moving fault, and hence by the power of these pulses and the energy they carry (Trifunac 2005; Gičev and Trifunac 2009a). Therefore, in this paper we select the excitation in terms of simple pulses, to simulate the actions of strong ground motion near faults.

Previous studies of nonlinear response of soils to incident earthquake waves have focused on the changes in peak amplitudes of ground motion (Trifunac and Todorovska 1996) and the changes in the site periods (Trifunac 2008). To understand how the energy of incident waves is absorbed during passage of large, near-field pulses, it is necessary to work with hysteretic models of soils and to consider nonlinear representations of wave motion, which allow creation of strain-localization zones in the soil. To begin to understand these phenomena, we have started to analyze such problems incrementally in terms of simple models based on numerical modeling of two-dimensional SH wave motion and bilinear representation of nonlinear deformations (Gičev and Trifunac 2009a). We first considered nonlinear deformations in the soil and relative energy absorption during 2-D SSI, when the foundation and the building are assumed to respond as continuous linear media (Gičev and Trifunac 2012). In this paper, we extend such analyses to (1) nonlinear soil and foundation, and (2) nonlinear soil and foundation with a thin, soft layer having low-yielding strain surrounding the foundation. In both cases, the building is assumed to respond in the linear range.

It is known from theoretical investigations of SSI that rigid foundations are efficient in the scattering of incident seismic waves, and that this scattering depends on the foundation shape and its relative stiffness (Wong and Trifunac 1974; Gičev 2005). While this scattered energy is smaller for actual foundations of buildings because those are never as rigid as their mathematical models (Trifunac et al. 1999), the scattering from flexible foundations still plays an important role in bringing about pockets of nonlinear soil deformation, which then lead to increased effective compliances and to their asymmetry. Observations of the response of full-scale structures during strong earthquake shaking show indirectly how prominent these nonlinearities in the soil-structure systems can be (Trifunac et al. 2001a,b). Observations also show that these nonlinear deformations in the soil usually occur well before any damage begins in the buildings. Since this natural energy-absorbing mechanism is beneficial for reducing the damage in the buildings, it should be studied and whenever possible incorporated into future design methods.

Nonlinear site response is a complex problem that involves many geometrical and material parameters in the description of the governing models, where extrapolations are at best very difficult due to the chaotic nature of large excitation and large nonlinear response. Hence, in the following our modest goal will be to illustrate what may occur in the presence of nonlinearities in the soil and in the foundation during SSI, while the building remains linear. Comprehensive sensitivity studies of how these results depend on all governing parameters are beyond the scope of this paper.

2. MODEL

During the wave passage, the soil, the foundation, and the structure can all undergo nonlinear deformations, and after the motion is over they can be left with permanent strains. Because the aim of this paper is to study only the nonlinear zones in the soil and in the foundation, those will be modeled as nonlinear, while the building will be forced to remain linear. The three variants of the model to be considered are shown in Figs. 1a and 1b. The model in Fig. 1a will be considered twice, first with linear and then with nonlinear deformations in the foundation. The incoming wave is taken to be a half-sine pulse of a plane SH wave, which is intended to model strong-motion pulses near faults. A dimensionless frequency $\eta = 2a/\lambda = a/\left(\beta_s \cdot t_{d0}\right)$ will be used as a measure of the pulse duration

(wavelength), where a is half the width of the foundation, λ is the wavelength of the incident wave, β_s is the shear-wave velocity in the soil, and t_{d0} is the duration of the pulse.

We will use the finite-difference model as described in Gičev and Trifunac (2012). To set up the grid spacing in the finite-difference representation of the model, the pulse is analyzed in the space domain(s), and the displacement in the points occupied by the pulse is $w(s) = A\sin[(\pi \cdot s/(\beta_s \cdot t_{d0})]$, where A is the amplitude of the pulse and s is the distance of the considered point to the wave front in initial time, in the direction of propagation. Using the fast Fourier transform, the half-sine pulse is transformed into wave number domain (k) as $w(k) = F[w(s)]$. The maximum response occurs for k = 0 (rigid-body motion). As k increases, the response decreases and diminishes toward zero as k approaches infinity. We selected the largest wave number to be considered in this analysis, $k = k_{max}$, for which the k-response is at least 0.03 of the maximum response (Gičev 2008). Then, for this value of k_{max}, the corresponding wavelengths and the corresponding frequencies are $\lambda_{min} = 2\pi / k_{max} = 2\pi\beta / \omega_{max}$.

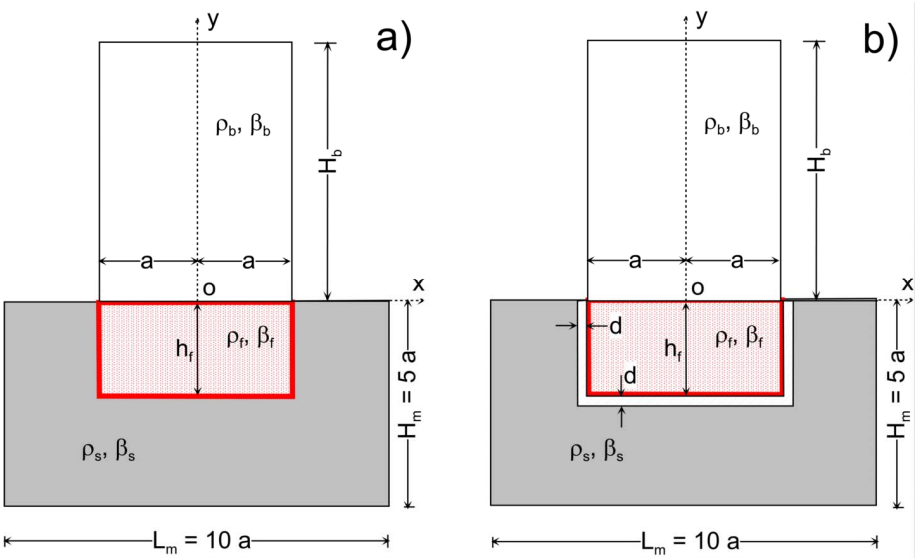

Figure 1. Nonlinear soil-flexible foundation-linear structure system: (a) linear or nonlinear foundation and nonlinear soil, (b) foundation surrounded by soft, nonlinear layer and nonlinear soil.

Accuracy of the finite difference (FD) grid depends on the ratio of the numerical and physical velocities of propagation, c/β, which ideally should be 1. The parameters that influence this accuracy are: (1) the density of the grid $m = \lambda / \Delta x$ (m is the number of points per wavelength λ, and Δx is the spacing between the grid points); (2) the Courant number, $\chi = \beta_s \Delta t / \Delta x$; and (3) the angle of the wave incidence, θ. It has been shown that the error increases when m decreases, χ decreases, and θ is close to 0 or $\pi/2$. For second-order approximation, it is recommended that $m \geq 12$ (Gičev 2008).

To model soil response numerically, we chose a rectangular soil box with dimensions $L_m = 10 \cdot a$ and $H_m = L_m / 2 = 5 \cdot a$ (Figs. 1a,b). For practical reasons, the maximum number of space intervals in the grid in the horizontal (x) direction is set at 250, and in the vertical (y) direction at 400 (125 in the soil

box and 275 in the building). The minimum spatial interval for this setup is $\Delta x_{\min} = L_m / 250 = 95.5/250 = 0.382\ m$. For a finer grid, the computational time increases rapidly. With this limitation in mind, and for $\eta = 2$, the largest wave number, $k_{\max}$, for which the response is greater than 3% of the maximum response, $F(k_0)$, has frequency $\omega_{\max} = 980\ rad/s$ (Gičev 2008). The shortest wavelength for shear-wave velocity in the soil $\beta_s = 250 m/s$ is then $\lambda_{\min} = 1.603\ m$, and the finest grid density is $m = \lambda_{\min} / \Delta x_{\min} = 1.603/0.382$. This corresponds to about 4 points / $\lambda_{\min} < m_{\min}$ for this wavelength. Our numerical scheme is $O(\Delta t^2, \Delta x^2)$, so we need at least m = 12 points/ $\lambda_{\min}$ to resolve the shortest wavelength, $\lambda_{\min}$. For $\eta = 2$, our grid cannot resolve the shortest wavelength when we have only 4 spatial grid points. This implies that the pulse should be low-pass filtered. A cut-off frequency $\omega_c = 200\ rad/s$ was chosen. Then $\lambda_{\min} = 7.854\ m$ and grid density $m = \lambda_{\min} / \Delta x_{\min} = 7.854/0.382 \approx 20$ points / $\lambda_{\min} > m_{\min}$. It can be shown that for $\eta = 0.5$ only a negligible amount of the total power is filtered out, while for $\eta = 2$ a considerable amount is filtered out. Also, it can be shown that for $\eta = 2$ the amplitude of the filtered pulse is smaller than the amplitude of the non-filtered pulse, which we chose to be A = 0.05 m, while for $\eta = 0.5$ the amplitude is almost equal to the amplitude of the non-filtered pulse. Numerical tests have shown that the viscous absorbing boundary rotated toward the middle of the foundation-building interface reflects only a negligible amount of energy back into the model (Gičev 2005; 2008).

For 2-D problems, the numerical scheme is stable if $\Delta t \le \min[(1/\Delta x^2 + 1/\Delta y^2)^{1/2} \beta]^{-1}$. We assume that the shear stress in the x direction depends only upon the shear strain in the same direction and is independent of the shear strain in the y direction. The motivation for this assumption comes from our simplified representation of layered soil, which is created by deposition (floods and wind) into more or less horizontal layers. The foundation and the soil are assumed to be ideally elasto-plastic. Further, it is assumed that the contact points between the soil and the foundation remain bonded during the analysis and that the contact cells remain linear, as does the zone next to the artificial boundary (the bottom four rows and the left-most and right-most four columns of points in the soil box in Figs. 1a,b).

For our problem, the system of three partial differential equations (for u, v, and w) describing the dynamic equilibrium of an elastic body is reduced to just one equation (because $u = v = \frac{\partial}{\partial z} = 0$). The abbreviations $\varepsilon_x = \varepsilon_{xz}$, $\sigma_x = \tau_{xz}$, $\varepsilon_y = \varepsilon_{yz}$, and $\sigma_y = \tau_{yz}$ will be used in the following. The Lax-Wendroff computational scheme is used for solving the governing equations (Gičev 2005).

3. ENERGY AND DISTRIBUTION OF PERMANENT STRAIN

In the following examples, we use the properties of the Holiday Inn hotel in Van Nuys, California to select the model properties of the building, and we consider the response in the east-west (longitudinal) direction only. This building was studied extensively using different models and representations (Gičev and Trifunac 2009b), and the body of those results can be used to complement future comparisons and interpretations of its response.

A question arises as to how to choose the yielding strain ε_m to study strain distribution in the system. The displacement, the velocity, and the linear strain in the soil (β_s = 250 m/s) during the passage of a

plane wave in the form of a half-sine pulse are $w = A\sin(\pi \cdot t / t_{d0})$, $v = \dot{w} = (\pi / t_{d0}) A\cos(\pi t / t_{d0})$, and $|\varepsilon| = v_{\max} / \beta_s = \pi A / (\beta_s t_{d0})$. If, for a given input plane wave, we choose the yielding strain ε_m multiplied by some constant between 1 and 2, the strains in both directions will remain linear before the wave reaches the free surface or the foundation, for any incident angle. This case can be called "intermediate nonlinearity." If we want to analyze only the nonlinearity due to scattering and radiating from the foundation, we should avoid the occurrence of the nonlinear strains caused by reflection from the half-space boundary. Then we may choose $\varepsilon_m \geq \max\left(\frac{2\pi A\sin\gamma}{\beta_s t_{d0}}; \frac{2\pi A\cos\gamma}{\beta_s t_{d0}}\right)$. We call this case "small nonlinearity." If the soil is allowed to undergo permanent strains due to wave passage of incident waves in the full space, then we may choose the maximum strain $\varepsilon_m < \max\left(\frac{\pi A\sin\gamma}{\beta_s t_{d0}}; \frac{\pi A\cos\gamma}{\beta_s t_{d0}}\right)$.

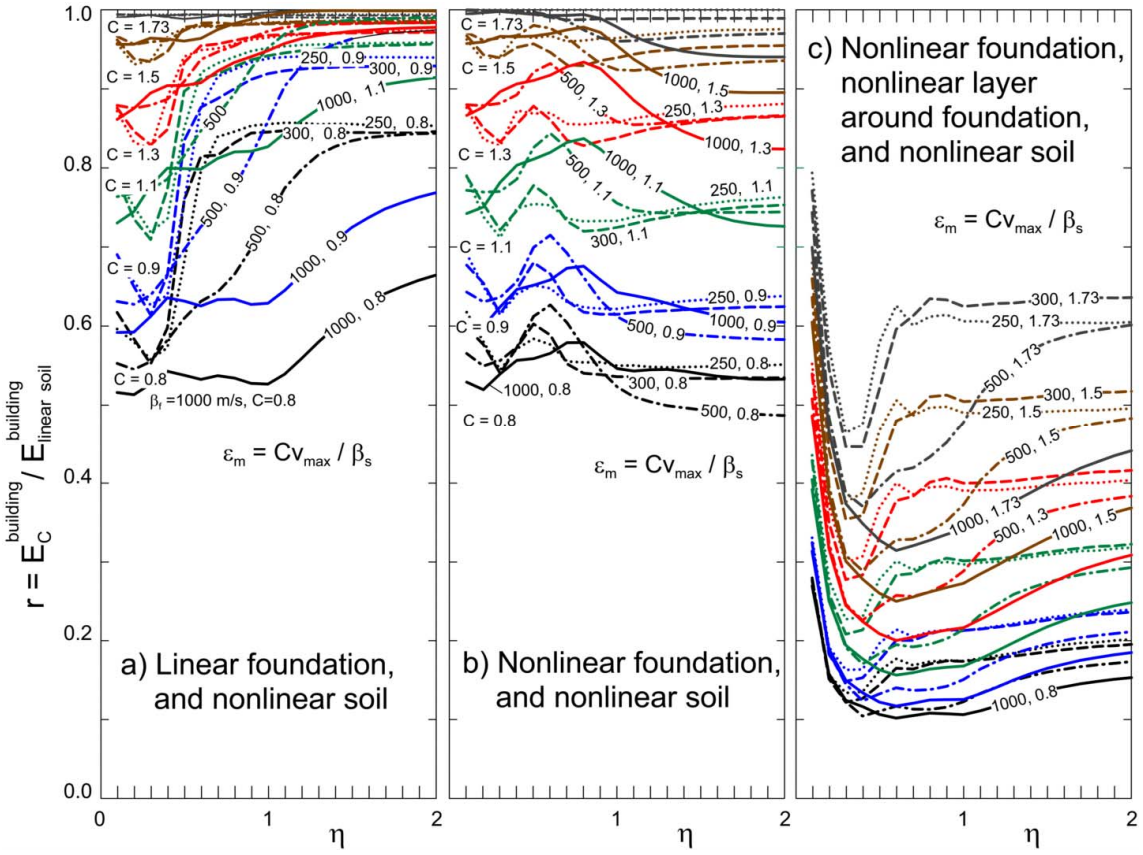

Figure 2. Reduction of wave energy entering the linear building for (a) linear foundation, (b) nonlinear foundation, and (c) nonlinear, soft layer surrounding the foundation, for different levels of soil nonlinearity (C = 0.8, 0.9, 1.1, 1.3, 1.5, and 1.73) and for different foundation rigidities through β_f = 250, 300, 500, and 1000 m/s.

This condition guarantees that in either the x or y direction the soil will undergo permanent strains during the passage of the plane wave. Generally, the yielding strain can be written as $\varepsilon_m = Cv_{\max} / \beta_s = C\pi A / (\beta_s t_{d0})$, where C is a constant that controls the yielding stress (strain) in the soil. We then consider the following cases of nonlinearity, depending upon C (Gičev and Trifunac 2012):

- $C \geq 2$: Small nonlinearity. Nonlinear strain does not occur until the wave hits the foundation.
- $1 \leq C < 2$: Intermediate nonlinearity. Permanent strain does not occur until the wave is reflected from the free surface or from the foundation. Permanent strain will or will not occur after the reflection from the free surface, depending upon the angle of incidence.
- $C < 1$: Large nonlinearity. Permanent strain occurs after reflection from the free surface. Permanent strain may or may not occur before the wave reflects from the foundation.

4. ENERGY DISTRIBUTION IN THE SYSTEM

The energy flow through a given area can be defined, in terms of a plane-wave approximation, as $E_{in}^{a} = \rho_s \cdot \beta_s \cdot A_{sn} \int_0^{t_{d0}} v^2 \cdot dt$, where ρ_s and β_s are the density and shear-wave velocity in the soil, respectively, and v is a particle velocity. A_{sn} is the area (normal to the direction of the ray) through which the wave is passing. For our geometrical setting (Figs. 1a,b), the area normal to the wave passage is $A_{sn} = 2 \cdot H_m \cdot \sin\gamma + L_m \cdot \cos\gamma = L_m \cdot (\sin\gamma + \cos\gamma)$. Combining the above relations and integrating, the analytical solution for the input wave energy into the model becomes

$E_{in}^{a} = \rho_s \cdot \beta_s \cdot L_m \cdot (\sin\gamma + \cos\gamma) \cdot (\pi A / t_{d0})^2 \cdot t_{d0} / 2$. For the defined size of the soil island, L_m, and the defined angle of incidence, γ, the input energy is reciprocal with the duration of the pulse, which means it is a linear function of the dimensionless frequency η. Because for short pulses in our example calculations are low-pass filtered up to $\omega_c = 200\ rad/s$, the analytical and the numerical solutions for input wave energy will not coincide. Since our system is conservative, the input energy is balanced by:

- Cumulative energy going out from the model, E_{out}.
- Cumulative hysteretic energy (energy spent for creation and development of permanent strains in the soil), computed from:

$$E_{hys} = \sum_{t=0}^{T_{end}} \Delta t \cdot \sum_{i=1}^{N} \left(\sigma_{xi} (\Delta\varepsilon_{xpi} + 0.5 \cdot \Delta\varepsilon_{xei}) + \sigma_{yi} (\Delta\varepsilon_{ypi} + 0.5 \cdot \Delta\varepsilon_{yei}) \right),$$

  where T_{end} is the time at the end of the analysis; N is the total number of points; σ_{xi}, σ_{yi} are the stresses at point i in the x and y directions, respectively; $\Delta\varepsilon_{xpi} = \varepsilon_{xpi}^{t+\Delta t} - \varepsilon_{xpi}^{t}$ is the increment of the permanent strain in the x direction at point i; $\Delta\varepsilon_{ypi} = \varepsilon_{ypi}^{t+\Delta t} - \varepsilon_{ypi}^{t}$ is the increment of the permanent strain in the y direction at point i; $\Delta\varepsilon_{xei} = \varepsilon_{xei}^{t+\Delta t} - \varepsilon_{xei}^{t}$ is the increment of the elastic strain in the x direction at point i; and $\Delta\varepsilon_{yei} = \varepsilon_{yei}^{t+\Delta t} - \varepsilon_{yei}^{t}$ is the increment of the elastic strain in the y direction at point i.
- Instantaneous energy in the building, consisting of kinetic and potential energies, can be computed from:

$$E_b = E_k + E_p = 0.5 \cdot \Delta x \cdot \Delta y_b \cdot \sum_{i=1}^{N} \left(\rho \cdot v_i^2 + \mu \cdot (\varepsilon_x^2 + \varepsilon_y^2) \right).$$

This balance was discussed in Gičev (2008) for a semi-cylindrical foundation, a pulse with $\eta = 1.5$, for incident angle $\gamma = 30^0$, and a yielding strain defined by C = 1.5, and it will be assumed to hold here as well for the rectangular foundation.

To study only the effect of scattering from the foundation, following Gičev (2008) the building will be considered to be high enough so that the reflected wave from the top of the building cannot reach the building-foundation contact during the time of analysis. The analysis is terminated when the wave completely exits the soil island. In this paper, the hysteretic energy in the soil and the energy in the building are the subjects of interest. Gičev studied these two types of energy as functions of the dimensionless frequency η. For a semi-circular foundation, he showed that as the foundation becomes stiffer, a larger part of the input energy is scattered, and less energy enters the building.

Figures 2a, b, and c show the reduction of the energy entering the building relative to the case when the soil is linear. The results are shown for four different foundation stiffnesses expressed by way of β_f = 250, 300, 500, and 1000 m/s. If the soil is linear, the reduction multiplier is 1. Figure 2a is reproduced here from the work of Gičev and Trifunac (2012) to help in the comparison with the results shown in Figs. 2b and c. It presents results for the foundation, which always deforms in the linear range. Figure 2b shows the results for the foundation material allowed to deform nonlinearly. Figure 2c shows the results for a nonlinear foundation surrounded by a thin, nonlinear layer (Fig. 1b).

In Figs. 2, we illustrate the energy reduction for six values of C = 0.8, 0.9, 1.1, 1.3, 1.5, and 1.73, as follows for the case of nonlinear soil, linear foundation, and linear building (Fig. 2a). (1) For small nonlinearity (e.g., C = 1.73), the ratios $E_C^{building}$ (C = 1.73) / $E_{linear\ soil}^{building}$ (C = ∞) are close to one for every η, showing that the small nonlinearity in the soil does not reduce the energy entering the building significantly. (2) For intermediate nonlinearity (e.g., C = 1.5), the ratios $E_C^{building}$ (C = 1.5) / $E_{linear\ soil}^{building}$ (C = ∞) show that there is a small reduction of the energy entering the building with the smallest ratio r ~ 0.94 near η = 0.2 to 0.3 and for β_f = 250 m/s in Fig. 2a. The values of η = 0.2 to 0.3 correspond to the excitation with wavelengths 3 to 5 times longer than the width of the foundation, and this corresponds to the cases in which all points along the contact of soil and foundation are forced to move in phase and with similar amplitudes. With increasing η (larger than ~0.7), the reduction decreases, and the ratio r in Fig. 2a tends towards 1. (3) For big nonlinearity (e.g., C = 0.8), the ratios $E_C^{building}$ (C = 0.8) / $E_{linear\ soil}^{building}$ (C = ∞) show that the reduction of energy entering the building is significant for all considered values of foundation stiffness. The ratio r is the smallest for the stiffest considered foundation (β_f = 1000 m/s). Figure 2b shows that when the foundation experiences nonlinear deformations, the reduction of the high-frequency energy entering the building is further increased relative to the case when the foundation remains linear. Figure 2c shows significant energy absorption capacity of the thin, nonlinear layer surrounding the foundation.

The results computed for case (3) above are dependent upon the size of the model box. Before the wave reaches the foundation, it loses energy due to work spent for creation of permanent strains in the soil. But for our examples, this dependence turns out to be small. For example, as pointed out in Gičev and Trifunac (2012), for β_f = 250 m/s and η = 0.3, the case of linear soil gives $E_{linear\ soil}^{building}$ = 164,540 J. For soil box L_m = 10a wide and H_m = 5a deep, the energy entering the building is $E_C^{building}$ (C = 0.8) =

90,769 J, and the ratio r = 0.55. For a soil box $L_m = 20a$ wide and $H_m = 10a$ deep, the energy entering the building is $E_C^{building}$ (C = 0.8) = 88,884 J, and r = 0.54, which is about a 2% difference for a smaller (approximately 2 x 2) soil box. From this, one can conclude that if this extreme case $r_{\beta_f=250}(C=0.8,\eta=0.3) = r^{\min}_{\beta_f=250}(C=0.8,\eta)$ (see Fig. 2a) gives only a 2% difference, at other values of η we will obtain even smaller differences due to different sizes of the model. However, if C becomes smaller (for larger nonlinearities) the dependence on the model size will become more pronounced.

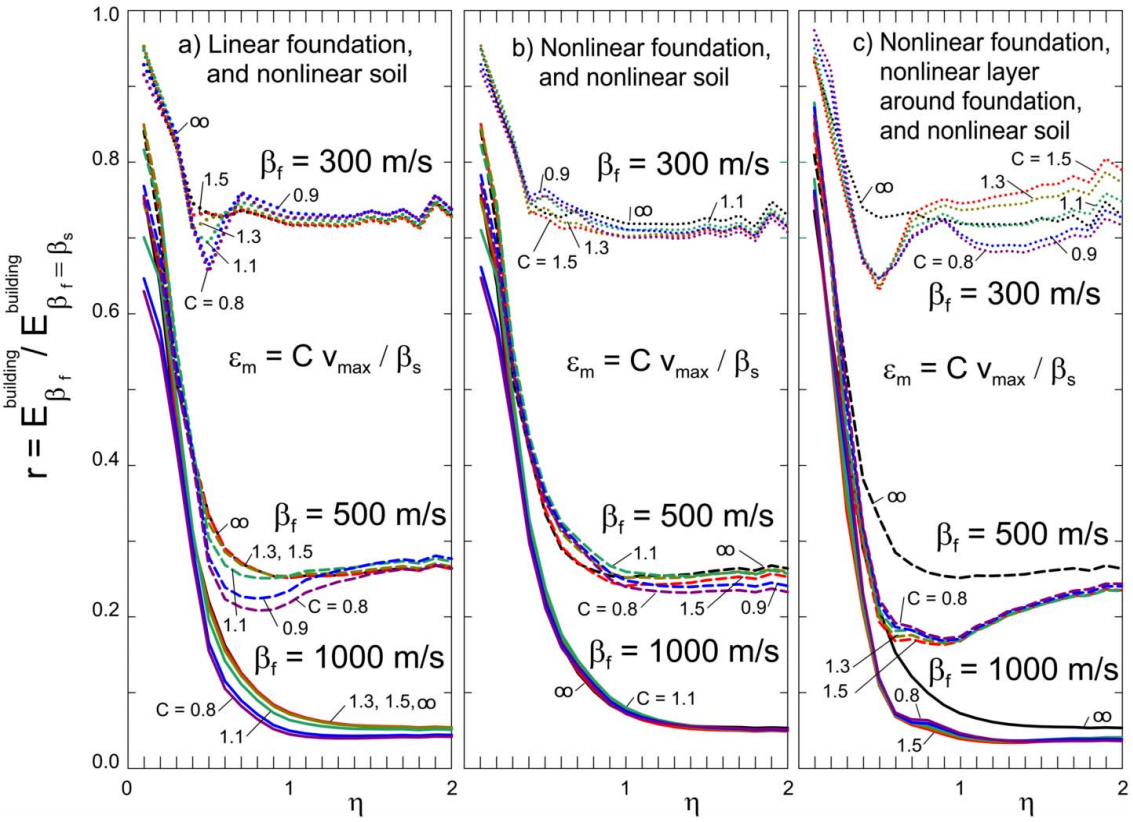

Figure 3. Reduction of wave energy by scattering, entering the linear building for (a) linear foundation, (b) nonlinear foundation, and (c) foundation surrounded by soft, nonlinear layer, for different levels of soil nonlinearity (C = 0.8, 0.9, 1.1, 1.3, 1.5, and ∞) and for different foundation rigidities expressed as β_f = 300, 500, and 1000 m/s.

Next, we illustrate how the level of the nonlinearity affects the level of scattering. This is shown in Figs. 3a, b, and c. It is seen that the scattering does not depend much on the level of nonlinearity in the soil for small and intermediate nonlinearities and is essentially the same as in the case of linear soil. For large nonlinearity, the effect becomes more significant. The examples in Figs. 3 show that the stiffness of the foundation is the key factor that determines how much energy is scattered from the foundation.

5. DISCUSSION AND CONCLUSIONS

The examples of nonlinear soil and foundation responses shown in this paper confirm that the energy entering a building can be reduced significantly before the waves approach and then enter the building. Nonlinear soil structure interaction is thus a far more efficient "base isolation" system than what can be accomplished by installing base isolators at the foundation level or somewhere within the structure. Clearly, it is better to (1) absorb energy before it enters the foundation and the structure, and (2) absorb it in the soil, which has far more powerful absorbing capacity than any isolator because it can accommodate large volumes with nonlinear deformations. Finally, the energy absorption by nonlinear soil response is cheap and maintenance free.

Nature has already provided us with such a powerful base isolation system, as evidenced by the documented reduction of damage to the buildings during the 1994 Northridge (Trifunac and Todorovska 1998) and 1933 Long Beach earthquakes (Trifunac 2003). Such reductions obviously also occurred during many other earthquakes in spite of the fact that those may not have been documented. However, as for any other energy-absorbing systems, the natural soil can also be an efficient and controllable energy sink only for a range of excitation amplitudes. This range will depend on many local conditions, and on the proximity to the moving fault and to the zones of extreme amplification of seismic waves. In terms of what has been learned following the Northridge earthquake, this useful range might extend to peak ground velocities of 150 to 200 cm/s (Trifunac and Todorovska 1998). Near and beyond these large, strong-motion amplitudes, the soil may begin to break into blocks that move independently on the liquefied substratum. The structures will then begin to be damaged and destroyed by large differential displacements and rotations of their foundation, due to deformations and forces larger than those resulting from shaking.

In a real three-dimensional setting, the nonlinear soil response is obviously far more complex than what has been illustrated in this paper, but the effects can be expected to be qualitatively the same. The challenge for the next generation of performance-based design methods will be to include the soil in the design of the complete building-soil system and to maximize its energy-absorption potential for incident strong-motion waves.

REFERENCES

Gičev, V. (2005). *Investigation of soil-flexible foundation-structure interaction for incident plane SH waves*. Ph.D. Dissertation, Dept. of Civil Engineering, Univ. Southern California, Los Angeles, CA.

Gičev, V. (2008). Soil-structure interaction in nonlinear soil. *Izgradnja* **62:12**, 555–566.

Gičev, V., and Trifunac, M.D. (2009a). Transient and permanent rotations in a shear layer excited by strong earthquake pulses. *Bull. Seism. Soc. Amer.* **99:2B**, 1391–1403.

Gičev, V., and Trifunac, M.D. (2009b). Rotations in a shear beam model of a seven-story building caused by nonlinear waves during earthquake excitation. *Structural Control and Health Monitoring* **16:4**, 460–482.

Gičev, V., and Trifunac, M.D. (2012). Asymmetry of nonlinear soil strains. *(Submitted for publication.)*

Gupta, I.D., and Trifunac, M.D. (1988). Order statistics of peaks in earthquake response. *J. Eng. Mechanics-ASCE* **114:10**, 1605–1627.

Todorovska, M.I., and Trifunac, M.D. (1997a). Distribution of pseudo spectral velocity during Northridge, California earthquake of 17 January 1994. *Soil Dynamics and Earthquake Eng*. **16:3**, 173–192.

Todorovska, M.I., and Trifunac, M.D. (1997b). Amplitudes, polarity and time of peaks of strong ground motion during the 1994 Northridge, California earthquake. *Soil Dynamics and Earthquake Eng*. **16:4**, 235–258.

Todorovska, M.I., and Trifunac, M.D. (1998). Discussion of "The role of earthquake hazard maps in loss estimation: a study of the Northridge earthquake," by R.B. Olshansky. *Earthq. Spectra*. **14:3**, 557–563.

Trifunac, M.D. (1995). Empirical criteria for liquefaction in sands via standard penetration tests and seismic wave energy. *Soil Dynamics and Earthquake Eng*. **14:6**, 419–426.

Trifunac, M.D. (2003). Nonlinear soil response as a natural passive isolation mechanism, Paper II—the 1933, Long Beach, California earthquake. *Soil Dynamics and Earthquake Eng*. **23:7**, 549–562.

Trifunac, M.D. (2005). Power design method. Proc. of *Earthquake Engineering in the 21st Century to Mark 40th Anniversary of IZIIS— Skopje*, August 28–Sptember 1, 2005, Skopje and Ohrid, Macedonia.

Trifunac, M.D. (2008). The nature of site response during earthquakes, Proc. NATO ARW Workshop in Borovec, 30 Aug.–3 Sept. 2008, Bulgaria. In *Coupled Site and Soil-Structure Interaction Effects with Applications to Seismic Risk Mitigation* (T. Schantz and R.Iankov editors), NATO Science for Peace and Security Ser. C: Environmental Security, 3–31, Springer Science + Business Media, B. V. 2009.

Trifunac, M.D., and Todorovska, M.I. (1996). Nonlinear soil response—1994 Northridge, California, earthquake. *J. of Geotechnical Eng.*, ASCE **122:9**, 725–735.

Trifunac, M.D., and Todorovska, M.I. (1997a). Northridge, California, earthquake of 1994: Density of red-tagged buildings versus peak horizontal velocity and intensity of shaking. *Soil Dynamics and Earthquake Eng*. **16:3**, 209–222.

Trifunac, M.D., and Todorovska, M.I. (1997b). Northridge, California, earthquake of 17 January 1994: Density of pipe breaks and surface strains. *Soil Dynamics and Earthquake Eng*.. **16:3**, 193–207.

Trifunac, M.D., and Todorovska, M.I. (1998). Nonlinear soil response as a natural passive isolation mechanism—the 1994 Northridge, California, earthquake, *Soil Dyn. and Earthquake Eng.*, **17:1**, 41–51.

Trifunac, M.D., and Todorovska, M.I. (2004). 1971 San Fernando and 1994 Northridge, California, earthquakes: did the zones with severely damaged buildings reoccur? *Soil Dyn. and Earthquake Eng.* **24:3**, 225–239.

Trifunac, M.D., Todorovska, M.I., and Ivanović, S.S. (1994). A note on distribution of uncorrected peak ground accelerations during the Northridge, California, earthquake of 17 January 1994. *Soil Dynamics and Earthquake Eng*. **13:3**, 187–196.

Trifunac, M.D., Todorovska, M.I., and Ivanović, S.S. (1996). Peak velocities, and peak surface strains during Northridge, California, earthquake of 17 January 1994, *Soil Dyn. and Earthquake Eng*., **15:5**, 301–310.

Trifunac, M.D., Ivanović, S.S., and Todorovska, M.I. (2001a). Apparent periods of a building I: Fourier analysis, *J. of Struct. Engrg*, ASCE. **127:5**, 517–526.

Trifunac, M.D., Ivanović, S.S., and Todorovska, M.I. (2001b). Apparent periods of a building II: time-frequency analysis. *J. of Struct. Engrg*, ASCE **127:5**, 527–537.

Trifunac, M.D., Ivanović, S.S., Todorovska, M.I., Novikova, E.I., and Gladkov, A.A. (1999). Experimental evidence for flexibility of a building foundation supported by concrete friction piles. *Soil Dynamics & Earthquake Engrg.* **18:3**, 169–187.

Wong, H.L., and Trifunac, M.D. (1974). Interaction of a shear wall with the soil for incident plane SH-waves: elliptical rigid foundation. *Bull. Seism. Soc. Amer.* **64:6**, 1825–1842.